Carbonaceous Aerosols Recorded in a Southeastern Tibetan Glacier: Analysis of Temporal Variations and Model Estimates of Sources and Radiative Forcing

Mo Wang[1,2], Baiqing Xu[1], Junji Cao[3], Xuexi Tie[3,4], Hailong Wang[2], Rudong Zhang[5,2], Yun Qian[2], Philip J. Rasch[2], Shuyu Zhao[3], Guangjian Wu[1], Huabiao Zhao[1], Daniel R. Joswiak[1], Jiule Li[1], Ying Xie[1]

[1]*Key Laboratory of Tibetan Environment Changes and Land Surface Processes, Institute of Tibetan Plateau Research, Chinese Academy of Sciences, Beijing 100101, China;*

[2]*Atmospheric Sciences and Global Change Division, Pacific Northwest National Laboratory (PNNL), Richland, WA 99352, USA;*

[3]*State Key Laboratory of Loess and Quaternary Geology, Institute of Earth Environment, Chinese Academy of Sciences, Beijing 100085, China;*

[4]*National Center for Atmospheric Research, Boulder, CO, 80303, USA;*

[5]*Key Laboratory for Semi-Arid Climate Change of the Ministry of Education, College of Atmospheric Sciences, Lanzhou University, Lanzhou 730000, Gansu, China*

Corresponding author: Mo Wang

Email: wangmo@itpcas.ac.cn

Abstract. High temporal resolution measurements of black carbon (BC) and organic carbon (OC) covering the time period of 1956-2006 in an ice core over the southeastern Tibetan Plateau show a distinct seasonal dependence of BC and OC with higher respective concentrations but lower OC/BC ratio in the non-monsoon season than during the summer monsoon. We use a global aerosol-climate model, in which BC emitted from different source regions can be explicitly tracked, to quantify BC source-receptor relationships between four Asian source regions and the southeastern Tibetan Plateau as a receptor. The model results show that South Asia has the largest contribution to the present-day (1996-2005) mean BC deposition at the ice core drilling site during the non-monsoon season (October to May) (81%) and all year round (74%), followed by East Asia (14% to the non-monsoon mean and 21% to the annual mean). The ice-core record also indicates stable and relatively low BC and OC deposition fluxes from late 1950s to 1980, followed by an overall increase to recent years. This trend is consistent with the BC and OC emission inventories and the fuel consumption of South Asia (as the primary contributor to annual mean BC deposition). Moreover, the increasing trend of OC/BC ratio since the early 1990s indicates a growing contribution of coal combustion and/or biomass burning to the emissions. The estimated radiative forcing induced by BC and OC impurities in snow has increased since 1980, suggesting an increasing potential influence of carbonaceous aerosols on the Tibetan glacier melting and the availability of water resources in the surrounding regions. Our study indicates that more attention to OC is merited because of its non-negligible light absorption and the recent rapid increases evident in the ice core record.

Keywords

Carbonaceous aerosol, Tibetan glacier, Emissions, Radiative forcing

1. Introduction

Carbonaceous aerosol, released from fossil fuel, biofuel and/or biomass combustion, contains both black carbon (BC, a.k.a. elemental carbon, EC), a strong light absorber, and organic carbon (OC), which also absorbs in the near infrared, but more weakly than BC (Kirchstetter et al., 2004; Bond et al., 2006). Often mixed with other aerosol species, BC impacts human health, crop yields and regional climate (Auffhammer et al., 2006; Tie et al., 2009), and is believed to be the second strongest climate warming forcing agent after carbon dioxide (Jacobson, 2001; IPCC, 2013).

Because of their high population density and relatively low combustion efficiency, developing countries in South and East Asia such as India and China are hotspots of carbonaceous aerosol emissions (Ramanathan and Carmichael, 2008). During the cold and dry winter season, haze (heavily loaded with carbonaceous aerosols) builds up over South Asia, and exerts profound influences on regional radiative forcing (Ramanathan et al., 2007; Ramanathan and Carmichael, 2008), hydrologic cycles (Menon et al., 2002; Ramanathan et al., 2005), and likely Himalaya-Tibetan glacier melting that could be accelerated by the absorption of sunlight induced by BC in the air and deposited on the ice and snow surfaces (Ramanathan et al., 2007; Hansen and Nazarenko, 2004; Ming et al., 2013).

Due to the lack of long-term observations of emissions and concentrations of atmospheric carbonaceous aerosols, it is difficult to evaluate the effects of BC and OC on historical regional climate and environment before the satellite era. Some studies have evaluated historical anthropogenic emissions based on the consumption of fossil fuels and biofuels (Novakov et al., 2003; Ito and Penner, 2005; Bond et al., 2007; Fernandes et al., 2007). While fossil fuel is the major energy source in the urban areas of South Asia and East Asia, biomass combustion, such as fuel wood, agricultural residue and dung cake, is prevalent in rural areas (Revelle, 1976; Venkataraman et al., 2010; Street and Waldhoff, 1998). Biomass burning has been considered as the major source of black carbon emissions (Reddy and Venkataraman,

2002; Venkataraman et al., 2005). However, as reliable biomass consumption data are hard to obtain, estimates of BC and OC emissions from biomass burning are ambiguous and incomplete.

Measurements of carbonaceous aerosol concentrations in glacier ice are an ideal means to reconstruct historical emissions and reveal long-term trends of anthropogenic aerosol impacts on local climate. Greenland ice core measurements were previously used to reconstruct the North American BC emission history and its effects on surface radiative forcing back to the 1880s (McConnell et al., 2007). Himalayan ice cores retrieved from the Tibetan Plateau have revealed the mixed historical emissions from South Asia, Central Asia and the Middle East and also been used to evaluate radiative forcing from BC in snow (Ming et al., 2008; Kaspari et al., 2011). Using the Snow, Ice, and Aerosol Radiative (SNICAR) model, Flanner et al. (2007) estimated an instantaneous regional forcing of exceeding 20 W m^{-2} by BC in snow/glaciers over the Tibetan Plateau during the spring season.

By using five ice core records, Xu et al. (2009a) elucidated an important contribution of BC to the retreat of Tibetan glaciers in addition to greenhouse gases. Due to the short atmospheric lifetime of carbonaceous aerosols compared to greenhouse gases, emission reductions may be an effective way to mitigate their warming effects. Thus it is particularly important to identify the source regions and the source types of carbonaceous aerosols observed in Tibetan glaciers. Xu et al. (2009a) suggested that BC deposited on Tibetan Plateau was broadly from Europe and Asia. However, they didn't perform in-depth analysis on emissions from more specific source regions and the source types. In this study, we use the ice core retrieved from the southeastern Tibetan Plateau, also known as the Zuoqiupu ice core in Xu et al. (2009a), to reconstruct the history of atmospheric deposition of carbonaceous aerosols in this glacier, and to characterize emissions and source-receptor relationships with the help of a global climate model in which BC emitted from different source regions can be explicitly tracked. We also estimate the

respective contributions from BC and OC to radiative forcing in the Zuoqiupu glacier using the ice core measurements and the SNICAR model.

2. Methods

2.1 Measurements of carbonaceous aerosols in ice core

Zuoqiupu glacier is in the southeastern Kangri Karpo Mountains, located at the southeastern margin of the Tibetan Plateau (Figure 1). In 2007, an ice core of 97 meters in depth (9.5 cm in diameter) was retrieved within the accumulation zone of Zuoqiupu glacier at 96.92°E, 29.21°N, 5600 m a.s.l. The ice core was kept frozen and transported to laboratory facilities at the Institute of Tibetan Plateau Research (Lhasa branch) for analysis. The annual accumulation of snow/ice at the drill site was around 2 meters on average. The oxygen isotope ($\delta^{18}O$) samples were cut at 10 cm internals, and BC and OC samples at 10-25 cm, resulting in 18 and 9 samples per year on average, respectively. Thus this ice core provided a high temporal-resolution of $\delta^{18}O$, and BC and OC concentrations. BC and OC concentrations were measured by using a Desert Research Institute (DRI) Model 2001 Thermal/Optical Carbon Analyzer following the IMPROVE TOR protocol (Chow et al. 1993; Chow and Watson 2002; Cao et al. 2008). Note that according to the thermal/optical measurement method, the analytical result is technically called “EC”. Herein we use “BC” to be consistent with the notation in our model simulations and in the literature. The reported OC concentrations from the ice-core measurements can only account for water-insoluble part of OC in the ice samples because most of the water-soluble part cannot be captured by the filter-based method applied to liquid samples (melted from the ice). Further details on the analysis methods, ice core dating and calculation of BC and OC seasonal deposition fluxes can be found in Xu et al. (2009a).

2.2 Model and experimental setup

We use the Community Atmosphere Model version 5 (CAM5; Neale et al., 2012) to help understand the emissions, transport and dry/wet deposition of carbonaceous aerosols in the atmosphere. In the default aerosol scheme of CAM5, BC and primary OC are emitted into an accumulation size mode, where they immediately mix with co-existing hygroscopic species such as sulfate and sea salt (Liu et al., 2012). Hygroscopic aerosol particles in the accumulation mode are subject to wet removal by precipitation. Recent model improvements to the representation of aerosol transport and wet removal in CAM5 by Wang et al. (2013) have substantially improved the global distribution of aerosols, particularly, over remote regions away from major sources. To minimize the model biases in simulating meteorological conditions and, particularly, circulations that are critical to aerosol transport, we configure the CAM5 model to run in an offline mode (Ma et al., 2013) with wind, temperature, surface fluxes and pressure fields constrained by observations. However, cloud/precipitation fields and interactions between aerosol and clouds are allowed to evolve freely. A source tagging technique has been recently implemented in the CAM5 model to allow for explicitly tracking aerosols emitted from individual source regions and, therefore, assists in quantitatively characterizing source-receptor relationships (Wang et al., 2014). This tagging technique along with the CAM5 model is used in the present study to do source attribution for carbonaceous aerosols deposited to the Zuoqiupu glacier.

We conducted an 11-year (1995-2005) CAM5 simulation at horizontal grid spacing of 1.9° × 2.5° and 56 vertical levels, with prescribed sea surface temperatures and sea ice distribution. Reanalysis products from NASA Modern Era Retrospective-Analysis for Research and Applications (MERRA) (Rienecker et al., 2011) are used to constrain the meteorological fields of CAM5. For aerosols (including OC, BC and other important species), we use the year-2000 monthly mean emissions described by Lamarque et al. (2010) that have been used in many global climate models for present-day climate simulations, included in the fifth

assessment report (AR5) by the Intergovernmental Panel on Climate Change (IPCC). The monthly mean emissions are repeatedly used for each year in the 11-year simulation. Note that we do not intend to design the model experiment to simulate the whole historical record of BC in the ice core, but rather for a period of time to demonstrate the impact of meteorology (and associated transport and removal of aerosols) on the seasonal dependence of BC deposition in the target region and the lack of longer-term trend in deposition without considering the temporal variation of emissions.

As the ice core drill site was located at a remote and elevated area over the southeastern Tibetan Plateau, where local emissions are minimal. Deposition of carbonaceous aerosols is most likely contributed by the non-local major emission sources (e.g., distributions of mean BC emissions during non-monsoon and monsoon seasons shown in Figure 2) in South Asia and East Asia. These two regions, along with Southeast Asia and Central Asia, are identified as the potential source contributors. Thus BC emissions from the four regions and the rest of the world are explicitly tracked in the CAM5 simulation.

3. Results and Discussion

3.1 Seasonal dependence of carbonaceous aerosols

BC and OC concentrations in the Zuoqiupu ice core both exhibit statistically significant seasonal variations at the 0.05 level corresponding to the stable oxygen isotope variability, which shows high values during the winter and low values during the summer (Xu et al., 2009a). As shown in Figure 3, concentrations of BC and OC have distinct differences between the summer monsoon and non-monsoon seasons. Seasonally varying emissions and meteorological conditions that determine the transport pathways of BC and OC emitted from major sources, removal during the transport, and local precipitation rate can cause the seasonal variations of BC and

OC in ice at the sampling site. The seasonal dependence of BC and OC in ice core is consistent with available observations of atmospheric aerosols in the south slope of the Himalayas and the southeastern Tibetan Plateau, where the high concentration of carbonaceous aerosols during the cold and dry season was suggested to associate with the South Asian haze (Cong et al., 2009; Marinoni et al., 2010; Kaspari et al., 2011; Zhao et al., 2013a; Zhao et al., 2013b). The consistency between the seasonal dependence of airborne BC and OC concentrations and the seasonal variation of ice-core measurements indicates that seasonal differences in local precipitation rate is less likely to be the determining factor. Our model results (details discussed in the section 3.2) suggest that the seasonal dependence of BC deposition flux in the target region could be mainly due to meteorological conditions (and associated transport pathways and wet removal processes). The small seasonal contrasts in BC emissions from the major source regions (see Table 1) that are used in the model simulation do not seem to be able to explain the large seasonal difference in BC deposition, although the BC emissions are known to have large uncertainties.

Our further analysis shows that the ratio of OC to BC also has clear seasonal dependence. In Figure 3, the slope of the fitted line to measured OC versus BC concentrations during monsoon season is ~6.3, which is twice the slope for non-monsoon season (~3.2). The analysis of covariance (ANCOVA) for slope differences of single linear regressions of OC against BC between monsoon and non-monsoon seasons indicates that the seasonal dependence of the relationship between the concentrations of OC and BC is significant (at the 0.05 significance level). This also agrees with measurements derived from the ice core drilled from the Palong-Zanbu No. 4 Glacier (Xu et al., 2009b) and in atmospheric samples collected from Lulang, southeastern Tibetan Plateau (Zhao et al., 2013b). The seasonal dependence of the OC/BC ratio can possibly be derived from the seasonal sources of carbonaceous particles, circulation strength, transport pathways, and/or atmospheric deposition processes. Compared to the respective BC and OC

concentrations, the seasonal dependence of OC/BC ratio is less straightforward to understand. Circulation patterns together with wet removal processes still determine the transport pathways of emissions from major BC and OC source regions to the sampling site, which however are less likely to change OC/BC ratio from certain sources. Therefore, it is more plausible due to seasonally dependent contributions from source regions and/or emission sectors (including fuel types, quantity, and combustion conditions). Cao et al. (2005) found that the average OC/BC ratios measured from plumes of residential biomass burning and coal combustion are substantially higher than from vehicle exhaust. Higher OC/BC ratio during summer monsoon might indicate more contributions from biomass and/or coal burning than fossil fuel combustion.

3.2 Source attribution

To quantitatively attribute the source of BC at the drilling site (as a receptor region), we use the CAM5 model with the BC source tagging capability to conduct an 11-year simulation, with the last 10 years (1996-2005) used for analysis. The surrounding area is divided into four source regions (see Table 1 and Figure 4): South Asia, East Asia, Southeast Asia and Central Asia. BC emissions from each of the four regions and the rest of the world are explicitly tracked, so that the fractional contributions by emissions from the individual source regions to BC deposition at the receptor region can be explicitly calculated. Figure 4 shows the spatial distribution of fractional contribution from the four source regions. BC deposition at the drilling site (indicated by the black box in Figure 4), which has a consistent seasonal dependence (i.e., more during the non-monsoon season; Figure 5) with ice core measurements, is predominately (over 95%) from South Asia and East Asia. The seasonal dependence of BC deposition is also consistent with a recent regional climate modeling study on BC deposition on the Himalayan snow cover from 1998 to 2008 (Ménégoz et al., 2014).

The 10-year (1996-2005) average wind fields (at the surface and 500 hPa from MERRA reanalysis datasets), as shown in Figure 2, indicate distinct circulation patterns during summer monsoon (June-September) and non-monsoon (October-May) season, which in part determine the seasonal dependence of transport of aerosols emitted from the different major sources. During the non-monsoon season, strong westerly dominates the transport from west to east at all levels. Emissions from northern India and central Asia can have influence on BC in the direct downwind receptor region over southeastern Tibetan Plateau. During the summer monsoon season, the westerly moves northward and the monsoon flow from Bay of Bengal at the surface and middle levels (e.g., 500hPa), coupled with the monsoon from Indochina peninsula and South China Sea, exert influence on BC in the receptor area. The strong monsoon precipitation removes BC from the atmosphere during the transport. The high Himalayas can partly block the further transport of emissions from South Asia to Tibetan Plateau, although small local topographical features such as the Yarlung Tsangpo River valley can provide a gate for the pollution to enter the inner Tibetan Plateau (Cao et al., 2010). Elevated emissions from the west (or northern part of South Asia) can take the pathways at middle and upper levels but they have minimal contribution to deposition. Therefore, BC emissions from East Asia play a relatively more important role affecting deposition at the Zuoqiupu site during the monsoon season.

The fractional contributions to 10-year mean BC deposition at the drilling site from the four tagged regions are summarized in Table 1. Results show that South Asia is the dominant contributor (~81%) during the non-monsoon season with ~14% from East Asia, while the contribution of East Asia (~56%) is larger than that of South Asia (~39%) during the monsoon season. For the annual mean BC deposition, South Asia (~75%) is the biggest contributor, followed by East Asia (~21%). Emissions from the central Asia and Southeast Asia regions have much smaller contributions (<3%) for all seasons. These results agree well with the short-term

source attribution study by Lu et al. (2012) using the Hybrid Single-Particle Lagrangian Integrated Trajectory (HYSPLIT) model.

For comparison, seasonal and annual mean BC emissions from the individual tagged source regions are also included in Table 1. Apparently, the contrast in strengths of regional emissions alone cannot explain their relative contributions to BC deposition at the sampling site, and the small seasonal variations in emissions are unlikely the cause of seasonal dependence of source attribution. Note that the BC emission inventory (Lamarque et al., 2010) used in CAM5 doesn't consider seasonal variations in anthropogenic emissions, which is likely to have introduced biases in the quantitative model estimates of seasonal dependence of contributions, but the relative importance of source regions should be robust.

3.3 Interannual variations and long-term trend

Based on annual snow accumulation and BC and OC concentrations derived from the ice record, the annual BC and OC deposition fluxes can be estimated, which are then used to examine the interannual variations and long-term trend in the fluxes and the ratio of OC/BC, as well as the relationship with emissions from the major contributor. As illustrated in Figure 6, from late 1950s to 1980, the BC and OC fluxes in the Zuoqiupu ice core are relatively low and stable in comparison to those after 1980. During the period 1956 to 1979, average fluxes are 9.1 and 28.7 mg m^{-2} a^{-1} for BC and OC, respectively. Both BC and OC fluxes began to show increasing trends from early 1980s. These trends continued in the early 1990s but started to drop in the mid-1990s, reaching a minimum in 2002 followed by a rapid increase. In 2006, BC and OC fluxes are 19.2 and 93.9 mg m^{-2} a^{-1}, respectively, which are two and three times the respective average fluxes before 1980. The five-year average OC/BC flux ratio is steady before 1990; however, it shows a continual increase afterwards and has been higher than the average value (3.2) for the period of 1956-1979 since mid-1990s (Figure 6). The 10-year CAM5 model

simulation, in which annual emissions are fixed but meteorological conditions vary, shows no increasing trend in BC and OC deposition fluxes (BC deposition shown in Figure 5), indicating that the increasing trend seen in the observations was not due to changes in meteorology.

As shown in the CAM5 model simulation, the annual mean atmospheric deposition of BC over southeastern Tibetan Plateau is mostly contributed by emissions from South Asia, particularly, in the non-monsoon season. The BC and OC deposition fluxes derived from the ice-core measurements may reflect changes in South Asian emissions to some extent. The temporal variations of BC and OC deposition fluxes (see Figure 6) are compared with the primary BC and OC emissions from fossil fuel and biofuel combustion in South Asia during 1955-2000 (Bond et al., 2007). BC and OC emissions during 1996-2010 from Lu et al. (2011) are also illustrated in Figure 6 to extend the emission data to cover the entire time period that the ice core data span. Note that the emission data from Lu et al. (2011) are only for India, which is the largest energy consumer and carbonaceous aerosol-emitting country in South Asia. There are differences between the emissions of Bond et al. and Lu et al. during the overlap time period (1996-2000). However, good agreements on the increasing trend can be found in the respective deposition fluxes and emissions of BC and OC (Figure 6). The OC/BC emission ratio also shows an increasing trend from the late 1990s to 2003, which is consistent with that of OC/BC ratio in the ice core record. The annual mean aerosol index over industrial and populated cities in the northern part of India increased from 1982-1993 and more significantly from 2000-2003 (Sarka et al., 2006). This trend is similar to that of carbonaceous aerosols in the ice core record, and it might indicate a causal relationship between BC and OC over southeastern Tibetan Plateau and emissions from north part of South Asia.

3.4 Emission source analyses

BC and OC in the atmosphere are co-emitted from a variety of natural and anthropogenic sources, including combustion of fossil fuel, biofuel and/or biomass burning. In general, open biomass burning typically produces more abundant OC (i.e., larger OC/BC ratio) compared to fossil fuel combustion due to a lower process temperature (Ducret and Cachier, 1992). The OC/BC ratio has often been used to discriminate fossil fuel combustion and biomass burning emissions in the atmosphere and in precipitation (Novakov et al., 2000; Stone et al., 2007; Ducret and Cachier, 1992; Xu et al., 2009b). For example, Cao et al. (2005) collected particulate matter samples from the plumes of residential biomass burning, coal combustion, and motor-vehicle exhaust sources, and analyzed OC and BC with DRI Thermal/Optical Carbon Analyzer (Model 2001). They reported average OC/BC ratios of 60.3, 12.0, and 4.1 for biomass burning, coal-combustion and vehicle exhaust, respectively. The increasing OC/BC ratios based on the ice core measurements since the early 1990s (Figure 6) suggest an expanded coal consumption and/or usage of biomass fuel, although the ratios might have been underestimated because water-soluble OC was not captured in the sample analyses. However, such bias would have occurred to all the samples and had little impact on the trend, unless including water-soluble OC could dominate the temporal variation of OC/BC ratio. Otherwise, our results indicate that the relative contribution of coal combustion and biomass burning to the carbonaceous particles deposited into the ice core in southeastern Tibetan Plateau has been increasing faster than the contribution of fossil fuel combustion since early 1990s. Improved combustion technologies may have reduced both BC and OC emissions from the combustion of the same amount of fuels, but the influence on OC/BC ratio is unclear. Presumably improved combustion technologies after 1990 in South and East Asia did not dominate the OC/BC ratio.

The temporal variations of BC and OC in the Zuoqiupu ice core, along with the source attribution analysis of the CAM5 model results, suggest an increasing trend

in emissions and altered emission sources in South Asia during the late 20th century. Coal has been the primary energy source in South Asia. For example, in India coal accounted for 41% of the total primary energy demand in 2007, followed by biomass (27%) and oil (24%) (IEA, 2009). The consumption data of coal and crude oil in South Asia (BP Group, 2009) is compared with the BC and OC fluxes in Figure 6 (bottom right). Coal consumption had an increasing trend from 1965 to 2008, particularly in the two time periods 1980-1995 and 2003-2008 after a level off during 1996-2002. This trend is consistent with the variations of BC and OC deposition fluxes in the Zuoqiupu ice core. The correlations between coal consumption and BC ($R^2 = 0.43$, $p < 0.001$) and OC ($R^2 = 0.62$, $p < 0.001$) in the ice core are both statistically significant. The oil consumption had a comparable increasing trend as coal before it slowed down during 2000-2006.

Biomass is the second largest energy resource in South Asia, and it is essential in rural areas. In India, 70% of the population lives in rural areas, and depends substantially on solid fuels (i.e., firewood, animal dung, and agriculture residues) for cooking and heating (Heltberg et al., 2000). Even in urban areas, biomass contributes to 27% of the household cooking fuel (Venkataraman et al., 2010). Although the consumption of biomass is lower than coal, the OC/BC emission ratio for biomass burning is much higher than from coal combustion (60.3 vs. 12.0) (Cao et al., 2005). BC emission factor for biomass burning (varying from 0.48 ± 0.18 g kg^{-1} for savanna and grassland burning to 1.5 g kg^{-1} for charcoal burning) is also generally higher than that for coal (0.2 g kg^{-1} for most combustion conditions) and oil combustion (0.3 g kg^{-1} on average, varying from 0.08 g kg^{-1} for heavy fuel oil to 0.66 g kg^{-1} for diesel) (Andreae and Merlet, 2001; Bond et al., 2004, 2007). Therefore, it is very likely that the OC/BC ratio of atmospheric carbonaceous aerosols and in the ice-core samples (Figure 6) was dominated by biomass burning emissions. Previous studies have concluded that carbonaceous aerosol emissions from biomass burning are the largest source in South Asia (Venkataraman et al.,

2005; Gustafsson et al., 2009). A general increase in energy-intensive life-styles associated with the accelerated growth of population and economy put pressure on energy resources, and induced energy transitions and use of non-sustainable biomass in South Asia (Sathaye and Tyler, 1991; Pachauri, 2004; Fernandes et al., 2007). For instance, biofuel consumption in South Asia increased by 21% per decade on average during 1950-2000 (Bond et al., 2007; Fernandes et al., 2007). In addition, fuel wood, a more desirable biofuel option, contributed 68% in 1978 to total energy demand by rural populations in India, and increased to 78% in 2000 (Fernandes et al., 2007).

3.5 Radiative forcing induced by carbonaceous aerosols in Tibetan Glaciers

BC is often the most important light-absorbing impurity in surface snow because of its strong absorption of solar radiation. Effect of BC in snow on surface albedo reduction and resultant positive radiative forcing have been widely addressed and reported (e.g., Warren and Wiscombe, 1980; Clarke and Noone, 1985; Hansen and Nazarenko, 2004; Hadley and Kirchstetter, 2012; Flanner et al., 2007; 2009; McConnell et al., 2007; Ming et al., 2008; Kaspari et al., 2011; Qian et al., 2011, 2014a,b). In contrast, the impact of OC in snow has not been widely assessed because of its relatively weak light-absorption over the entire spectrum compared to BC, and because of large uncertainties associated with OC light-absorbing properties and measurements of OC in snow. However, there have been increasing interests in light-absorbing OC (a.k.a. brown carbon) and its radiative effect in the atmosphere (e.g., Kirchstetter et al., 2004; Andreae and Gelencsér, 2006; Hoffer et al., 2006; Moosmüller et al., 2009; Yang et al., 2009; Lack and Cappa, 2010; Cheng et al., 2011). Hoffer et al. (2006) estimated that humus-like substances as part of OC from biomass burning contribute ~7% to the absorption over the entire spectrum, which is not negligible. Yang et al. (2009) highlighted that as the contribution to absorption from BC decreases towards the ultra violet wavelengths, absorption due

to brown carbon and dust becomes more significant, and they reported that at an observation site near Beijing brown carbon contributes over 10% to total absorption at mid-visible wavelengths. Thus the contribution of OC in snow to the surface albedo reduction is likely to be important, which has also been considered in recent climate modeling studies (Qian et al., 2014b).

In this study, we use the SNICAR-online model (available at http://snow.engin.umich.edu/; Flanner et al., 2007) to estimate radiative forcing induced by the observed BC and OC as if they were present in snow. Detailed description of the SNICAR model has been documented by Flanner and Zender (2005, 2006) and Flanner et al. (2007). Here we only briefly describe the setup of input parameters required for running the SNICAR model. A mass absorption cross-section (MAC) of 7.5 m^2 g^{-1} at 550 nm for uncoated BC particle and 0.6 m^2 g^{-1} for OC (Bond and Bergstrom, 2006; Kirchstetter et al., 2004; Yang et al., 2009) is assumed, and thus one of the input parameters for the online SNICAR model, MAC scaling factor, should be 1 for BC and 0.08 for OC. According to the previous studies (Cuffey and Paterson, 2010; Wiscombe and Warren 1980) and measurements in Qiyi glacier and Zuoqiupu glacier, an effective radius of 100 μm with density of 60 kg m^{-3} for new snow, and the effective radius of 400 μm with density of 400 kg m^{-3} for aged snow are adopted for the forcing calculation. As we focus on the estimation of radiative forcing by carbonaceous particles, other impurity contents, such as dust and volcanic ash, are set to be zero. The annual mean BC and OC concentrations during 1956-1979 was 4.4 ng g^{-1} and 13.8 ng g^{-1}, respectively, and they increased to 12.5 and 61.3 ng g^{-1} in 2006. As a consequence, the annual mean radiative forcing induced by BC (OC) in snow increases from 0.75 (0.20) W m^{-2} to 1.95 (0.84) W m^{-2}. Our estimate of mean BC forcing is lower than the estimated Eurasian radiative forcing (2.7 W m^{-2}) in spring (Flanner et al., 2009), but it's comparable to that in the East Rongbuk glacier over Himalayas, which was in the range of 1-2 W m^{-2} (Ming et al., 2008). Kaspari et al. (2009) reported a

three-fold increase in radiative forcing from BC in snow over Himalayas after 1975, which is consistent with the increasing trend in our results. Although BC concentration is one order of magnitude lower than OC, radiative forcing of BC is about two times larger than OC due to its much stronger absorption of solar radiation. Note that the MAC value of OC is highly spectral dependent (Kirchstetter et al., 2004; Hoffer et al., 2006; Barnard et al., 2008; Yang et al., 2009). It increases greatly towards shorter wavelengths. Consequently, the absorption of OC may be biased. It is also important to note that we didn't consider variations in chemical compounds of OC, or the changes of OC during sample filtration. Although the estimation of OC radiative forcing herein is rather crude, the increasing trend should be robust.

BC and OC concentrations in the ice core increased rapidly since 1980, and the induced radiative forcing rose as a consequence. According to the estimates using the SNICAR model, the average BC radiative forcing had increased 43% after 1980, and OC radiative forcing had an increase of 70%. These numbers are by no means accurate, but the stronger increasing trend in the ice core recorded OC than BC during 1990-2006 (Figure 6) suggests that the contribution of OC to the total radiative forcing in the glacier induced by snow/ice impurities deserves more attention.

4. Summary and Conclusions

Light-absorbing carbonaceous aerosols can induce significant warming in the atmosphere and in snow and glaciers, which likely accelerates the melting of glaciers over Himalayas and Tibetan Plateau. Ice-core measurement of carbonaceous aerosols is a useful mechanism for evaluating historical emission inventories and revealing long-term changes in anthropogenic aerosols and their impacts on regional climate. In this study, we analyze carbonaceous aerosols recorded in an ice core (97 meters in depth and 9.5 cm in diameter) retrieved from the Zuoqiupu glacier

(96.92°E, 29.21°N, 5600 m above sea level) in the southeastern Tibetan Plateau for their seasonal dependence and long-term trend. The glacier has a unique geographical location that is in close proximity to major Asian emission sources. With the help of a global climate model (CAM5) in which black carbon (BC) emitted from different source regions can be explicitly tracked, we are able to characterize BC source-receptor relationships between four Asian source regions (i.e., South Asia, East Asia, Southeast Asia and Central Asia) and the Zuoqiupu glacier area as a receptor. We also estimate the radiative forcing in snow due to BC and OC using the ice core measurements and an offline snow-ice-aerosol-radiation model (called SNICAR).

BC and OC concentrations in small segments of the Zuoqiupu ice core were measured using a thermal-optical method. Ice core dating based on significant seasonal variations of oxygen isotope ratios ($\delta^{18}O$) was used to construct the time series of BC and OC concentrations, which turned out to span the time period of 1956–2006. Not only do the concentrations of OC and BC in the ice core exhibit significant differences between the summer monsoon and non-monsoon seasons, which is likely due to changes in transport pathways and wet removal, but also the ratio of OC to BC shows a clear seasonal dependence that might be due to seasonal change in contributions from source regions and/or emission sectors. The CAM5 results show a similar seasonal dependence of BC and OC deposition to the glacier.

The MERRA reanalysis products used to drive the CAM5 model simulation show distinct circulation patterns during summer monsoon (June-September) and non-monsoon (October-May) seasons. Both the circulation patterns (and associated aerosol transport and wet removal) and seasonal variation of emissions in major source regions influence the seasonal deposition of aerosol at the Zuoqiupu site. The CAM5 simulation with tagged BC regional sources shows that South Asia is the dominant contributor (81%) to the 10-year mean BC deposition at the Zuoqiupu site during the non-monsoon season with 14% from East Asia, while the contribution of

East Asia (56%) is larger than that of South Asia (39%) during the monsoon season. For the annual mean BC deposition, South Asia (75%) is the biggest contributor, followed by East Asia (21%).

The annual mean BC and OC deposition fluxes into the ice core are also estimated to explore the interannual variations and long-term trends. Results show stable and relatively low BC and OC fluxes from late 1950s to 1979, followed by a steady increase through the mid-1990s. A more rapid increase occurred after the minimum in 2002. The BC and OC deposition fluxes in 2006 were two and three times the respective average before 1980.

The overall increasing trend in deposition fluxes since 1980 is consistent with the BC and OC emissions in South Asia as the major contributor. Moreover, the increasing trend of OC/BC ratio since early 1990s indicates a growth of the contribution of coal combustion and/or biomass burning to the carbonaceous aerosol emissions in the major contributing source regions, which is consistent with the trends in the consumption of coal, oil and biomass in South Asia.

Our offline calculation using the SNICAR model shows a significant increase of radiative forcing induced by the observed BC and OC in snow after 1980, which has implications for the Tibetan glacier melting and availability of water resources in the surrounding regions. More attention to OC is merited because of its non-negligible light absorption and the recent rapid increases evident in the ice core record.

Acknowledgements

This work was supported by the China National Funds for Distinguished Young Scientists and the National Natural Science Foundation of China, including 41125003, 41101063, 2009CB723901. H. Wang, Y. Qian and P.J. Rasch were supported by the U.S. Department of Energy (DOE), Office of Science, Biological and Environmental Research as part of the Earth System Modeling program. R. Zhang acknowledges support from the China Scholarship Fund. PNNL is operated

513 for DOE by Battelle Memorial Institute under contract DE-AC05-76RLO1830. The
514 National Center for Atmospheric Research is sponsored by the National Science
515 Foundation. We thank Zhongming Guo and Song Yang for providing the
516 observations of snow.

References

Andreae, M. O., and Merlet, P.: Emission of trace gases and aerosols from biomass burning, Global Biogeochem. Cy., 15, 955-966, doi: 10.1029/2000GB001382, 2001.

Auffhammer, M., Ramanathan, V., and Vincent, J. R.: Integrated model shows that atmospheric brown clouds and greenhouse gases have reduced rice harvests in India, Proc. Natl. Acad. Sci. USA, 103, 19668–19672, 2006.

Barnard, J. C., Volkamer, R., and Kassianov, E. I.: Estimation of the mass absorption cross section of the organic carbon component of aerosols in the Mexico City Metropolitan Area, Atmos. Chem. Phys., 8, 6665-6679, doi:10.5194/acp-8-6665-2008, 2008.

Bond, T. C. and Bergstrom, R. W.: Light absorption by carbonaceous particles: an investigative review, Aerosol. Sci. Tech., 40, 27–67, 2006.

Bond, T. C., Bhardwaj, E., Dong, R., Jogani, R., Jung, S., Roden, C., Street, D. G., and Trautmann, N. M.: Historical emissions of black and organic carbon aerosol from energy-related combustion, 1850–2000, Global Biogeochem. Cy., 21, GB2018, doi:10.1029/2006GB002840, 2007.

BP Group: BP Statistical Review of World Energy June 2009, Report, BP p.l.c., London, UK, 45 pp., 2009.

Cao, J. J., Wu, F., Chow, J. C., Lee, S. C., Li, Y., Chen, S. W., An, Z. S., Fung, K. K., Watson, J. G., Zhu, C. S., and Liu, S. X.: Characterization and source apportionment of atmospheric organic and elemental carbon during fall and winter of 2003 in Xi'an, China, Atmos. Chem. Phys., 5, 3127–3137, doi:10.5194/acp-5-3127-2005, 2005.

Cao, J., Tie, X., Xu, B., Zhao, Z., Zhu, C., Li, G., and Liu, S.: Measuring and modeling black carbon (BC) contamination in the SE Tibetan Plateau, J. Atmos. Chem., 67, 45–60, 2010.

Cao, J., Zhu, C., Chow, J., Liu, W., Han, Y., and Watson, J. G.: Stable carbon and oxygen isotopic composition of carbonate in fugitive dust in the Chinese Loess Plateau, Atmos. Environ., 42, 9118–9122, 2008.

Cheng, Y., He, K. B., Zheng, M., Duan, F. K., Du, Z. Y., Ma, Y. L., Tan, J. H., Yang, F. M., Liu, J. M., Zhang, X. L., Weber, R. J., Bergin, M. H., and Russell, A. G.: Mass absorption efficiency of elemental carbon and water-soluble organic carbon in Beijing, China, Atmos. Chem. Phys., 11(22), 11497-11510, doi:10.5194/acp-11-11497-2011, 2011.

Chow, J. C. and Watson, J. G.: $PM_{2.5}$ carbonate concentrations at regionally representative interagency monitoring of protected visual environment sites, J.

552 Geophys. Res, 107, 8344, doi:10.1029/2001JD000574, 2002.

553 Chow, J. C., Watson, J. G., Pritchett, L. C., Pierson, W. R., Frazier, C. A., and Purcell,
554 R. G.: The DRI thermal/optical reflectance carbon analysis system: description,
555 evaluation and applications in US air quality studies, Atmos. Environ., 27, 1185–1201,
556 1993.

557 Clarke, A. D. and Noone, K. J.: Soot in the Arctic snowpack: a cause for perturbations
558 in radiative transfer, Atmos. Environ., 19, 2045–2053, 1985.

559 Cong, Z., Kang, S., and Qin, D.: Seasonal features of aerosol particles recorded in
560 snow from Mt. Qomolangma (Everest) and their environmental implications, J.
561 Environ. Sci., 21, 914–919, 2009.

562 Cuffey, K. M. and Paterson, W. S. B. (Eds.): The physics of glaciers, Fourth Edition,
563 Academic Press, Burlington, USA, 2010.

564 Ducret, J. and Cachier, H.: Particulate carbon content in rain at various temperate and
565 tropical locations, J. Atmos. Chem., 15, 55–67, 1992.

566 Fernandes, S. D., Trautmann, N. M., Streets, D. G., Roden, C. A., and Bond, T. C.:
567 Global biofuel use, 1850–2000, Global Biogeochem. Cy., 21, GB2019,
568 doi:10.1029/2006GB002836, 2007.

569 Flanner, M. G. and Zender, C. S.: Linking snowpack microphysics and albedo
570 evolution, J. Geophys. Res., 111, D12208, doi:10.1029/2005JD006834, 2006.

571 Flanner, M. G. and Zender, C. S.: Snowpack radiative heating: influence on Tibetan
572 Plateau climate, Geophys. Res. Lett., 32, L06501, doi:10.1029/2004GL022076, 2005.

573 Flanner, M. G., Zender, C. S., Hess, P. G., Mahowald, N. M., Painter, T. H.,
574 Ramanathan, V., and Rasch, P. J.: Springtime warming and reduced snow cover from
575 carbonaceous particles, Atmos. Chem. Phys., 9, 2481-2497,
576 doi:10.5194/acp-9-2481-2009, 2009.

577 Flanner, M. G., Zender, C. S., Randerson, J. T., and Rasch, P. J.: Present-day climate
578 forcing and response from black carbon in snow, J. Geophys. Res., 112, D11202,
579 doi:10.1029/2006JD008003, 2007.

580 Gustafsson, Ö, Kruså, M., Zencak, Z., Sheesley, R. J., Granat, L., Engström, E.,
581 Praveen, P. S., Rao, P. S. P., Leck, C., and Rodhe, H.: Brown clouds over South Asia:
582 Biomass or fossil fuel combustion?, Science, 323, 495–497, 2009.

583 Hadley, O. L. and Kirchstetter, T. W.: Black-carbon reduction of snow albedo, Nat.
584 Clim. Change, 2, 437–440, 2012.

585 Hansen, J. and Nazarenko, L.: Soot climate forcing via snow and ice albedos, Proc.
586 Natl. Acad. Sci. USA, 101, 423–428, 2004.

587 Heltberg, R., Arndt, T. C., and Sekhar, N. U.: Fuelwood consumption and forest
588 degradation: a household model for domestic energy consumption in rural India, Land
589 Econ., 76, 213–232, 2000.

590 Hoffer, A., Gelencsér, A., Guyon, P., Kiss, G., Schmid, O., Frank, G. P., Artaxo, P.,
591 and Andreae, M. O.: Optical properties of humic-like substances (HULIS) in
592 biomass-burning aerosols, Atmos. Chem. Phys., 6, 3563-3570,
593 doi:10.5194/acp-6-3563-2006, 2006.

594 IEA: Chapter 9 – Country and regional profiles in the 450 Scenario, in: World Energy
595 Outlook 2009, International Energy Agency, France, 319–362, 2009.

596 IPCC: Climate Change 2013: The Physical Science Basis, Contribution of Working
597 Group I to the Fourth Assessment Report of the Intergovernmental Panel on Climate
598 Change, edited by Solomon, S., D. Qin, M. Manning, Z. Chen, M. Marquis, K.B.
599 Averyt, M. Tignor and H.L. Miller, Cambridge University Press, Cambridge, United
600 Kingdom and New York, NY, USA, 996 pp., 2013.

601 Ito, A. and Penner, J. E.: Historical emissions of carbonaceous aerosols from biomass
602 and fossil fuel burning for the period 1870–2000, Global Biogeochem. Cy., 19,
603 GB2028, doi:10.1029/2004GB002374, 2005.

604 Jacobson, M. Z.: Strong radiative heating due to the mixing state of black carbon in
605 atmospheric aerosols, Nature, 409, 695–697, 2001.

606 Kaspari, S. D., Schwikowski, M., Gysel, M., Flanner, M. G., Kang, S., Hou, S., and
607 Mayewski, P. A.: Resent increase in black carbon concentrations from a Mt. Everest
608 ice core spanning 1860–2000 AD, Geophys. Res. Lett., 38, L04703,
609 doi:10.1029/2010GL046096, 2011.

610 Kirchstetter, Thomas W., Novakov, T., and Hobbs, Peter V.: Evidence that the
611 spectral dependence of light absorption by aerosol is affected by organic carbon, J.
612 Geophys. Res., 109, D21208, doi:10.1029/2004JD004999, 2004.

613 Lack, D. A., and Cappa, C. D.: Impact of brown and clear carbon on light absorption
614 enhancement, single scatter albedo and absorption wavelength dependence of black
615 carbon, Atmos. Chem. Phys., 10, 4207-4220, doi:10.5194/acp-10-4207-2010, 2010.

616 Lamarque, J.-F., Bond, T. C., Eyring, V., Granier, C., Heil, A., Klimont, Z., Lee, D.,
617 Liousse, C., Mieville, A., Owen, B., Schultz, M. G., Shindell, D., Smith, S. J.,
618 Stehfest, E., Van Aardenne, J., Cooper, O. R., Kainuma, M., Mahowald, N.,
619 McConnell, J. R., Naik, V., Riahi, K., and van Vuuren, D. P.: Historical (1850–2000)

620 gridded anthropogenic and biomass burn ing emissions of reactive gases and aerosols:
621 methodology and application, Atmos. Chem. Phys., 10, 7017–7039,
622 doi:10.5194/acp-10-7017-2010, 2010.

623 Liu, X., Easter, R. C., Ghan, S. J., Zaveri, R., Rasch, P., Shi, X., Lamarque, J.-F.,
624 Gettelman, A., Morrison, H., Vitt, F., Conley, A., Park, S., Neale, R., Hannay, C.,
625 Ekman, A. M. L., Hess, P., Mahowald, N., Collins, W., Iacono, M. J., Bretherton, C.
626 S., Flanner, M. G., and Mitchell, D.: Toward a minimal representation of aerosols in
627 climate models: description and evaluation in the Community Atmosphere Model
628 CAM5, Geosci. Model Dev., 5, 709–739, doi:10.5194/gmd-5-709-2012, 2012.

629 Lu, Z., Streets, D. G., Zhang, Q., and Wang, S.: A novel back-trajectory analysis of
630 the origin of black carbon transported to the Himalayas and Tibetan Plateau during
631 1996–2010, Geophys. Res. Lett., 39, L01809, doi:10.1029/2011GL049903, 2012.

632 Lu, Z., Zhang, Q., and Streets, D. G.: Sulfur dioxide and primary carbonaceous
633 aerosol emissions in China and India, 1996–2010, Atmos. Chem. Phys., 11, 9839–
634 9864, doi:10.5194/acp-11-9839-2011, 2011.

635 Ma, P.-L., Rasch, P. J., Wang, H., Zhang, K., Easter, R. C., Tilmes, S., Fast, J. D., Liu,
636 X., Yoon, J.-H., and Lamarque, J.-F.: The role of circulation features on black carbon
637 transport into the Arctic in the Community Atmosphere Model Version 5 (CAM5), J.
638 Geophys. Res.-Atmos., 118, 4657–4669, 2013.

639 Marinoni, A., Cristofanelli, P., Laj, P., Duchi, R., Calzolari, F., Decesari, S., Sellegri,
640 K., Vuillermoz, E., Verza, G. P., Villani, P., and Bonasoni, P.: Aerosol mass and
641 black carbon concentrations, a two year record at NCO-P (5079 m, Southern
642 Himalayas), Atmos. Chem. Phys., 10, 8551–8562, doi:10.5194/acp-10-8551-2010,
643 2010.

644 McConnell, J., Edwards, R. L., Kok, G. L., Flanner, M. G., Zender, C. S., Saltzman, E.
645 S., Banta, J. R., Pasteris, D. R., Carter, M. M., and Kahl, J. D. W.: 20th century
646 industrial black carbon emissions altered Arctic climate forcing, Science, 317, 1381–
647 1384, 2007.

648 Ménégoz, M., Krinner, G., Balkanski, Y., Boucher, O., Cozic, A., Lim, S., Ginot, P.,
649 Laj, P., Gallée, H., Wagnon, P., Marinoni, A., and Jacobi, H. W.: Snow cover
650 sensitivity to black carbon deposition in the Himalayas: from atmospheric and ice
651 core measurements to regional climate simulations, Atmos. Chem. Phys., 14, 4237–
652 4249, doi:10.5194/acp-14-4237-2014, 2014.

653 Menon, S., Hansen, J., Nazarenko, L., and Luo, Y.: Climate effects of black carbon
654 aerosols in China and India, Science, 297, 2250–2253, 2002.

655 Ming, J., Cachier, H., Xiao, C., Qin, D., Kang, S., Hou, S., and Xu, J.: Black carbon

record based on a shallow Himalayan ice core and its climatic implications, Atmos. Chem. Phys., 8, 1343–1352, doi:10.5194/acp-8-1343-2008, 2008.

Ming, J., Xiao, C., Du, Z., and Yang, X.: An overview of black carbon deposition in High Asia glaciers and its impacts on radiation balance, Adv. Water Resour., 55, 80-87, doi:10.1016/j.advwatres.2012.05.015, 2013.

Moosmüller, H., Chakrabarty, R. K., and Arnott, W. P.: Aerosol light absorption and its measurement: A review, Journal of Quantitative Spectroscopy and Radiative Transfer, 110, 844-878, doi:10.1016/j.jqsrt.2009.02.035, 2009.

Neale, R. B., Chen, C.-C., Gettelman, A., Lauritzen, P. H., Park, S., Williamson, D. L., Conley, A. J., Garcia, R., Kinnison, D., Lamarque, J.-F., Marsh, D., Mills, M., Smith, A. K., Tilmes, S., Vitt, F., Cameron-Smith, P., Collins, W. D., Iacono, M. J., Easter, R. C., Ghan, S. J., Liu, X., Rasch, P. J., and Taylor, M. A.: Description of the NCAR Community Atmosphere Model (CAM 5.0), NCAR/TN-486+STR, available at: http://www.cesm.ucar.edu/models/cesm1.0/cam/docs/description/cam5_desc.pdf (last access: 25 November 2014), 2012.

Novakov, T., Andreae, M. O., Gabriel, R., Kirchstetter, T. W., Mayol-Bracero, O. L., and Ramanathan, V.: Origin of carbonaceous aerosols over the tropical Indian Ocean: Biomass burning or fossil fuels, Geophys. Res. Lett., 27, 4061–4064, 2000.

Novakov, T., Ramanathan, V., Hansen, J. E., Kirchstetter, T. W., Sato, M., Sinton, J. E., and Sathaye, J. A.: Large historical changes of fossil-fuel black carbon aerosols, Geophys. Res. Lett., 30, 1324, doi:10.1029/2002GL016345, 2003.

Pachauri, R. K.: The future of India's economic growth: the natural resources and energy dimension, Futures, 36, 703–713, 2004.

Qian, Y., Flanner, M. G., Leung, L. R., and Wang, W.: Sensitivity studies on the impacts of Tibetan Plateau snowpack pollution on the Asian hydrological cycle and monsoon climate, Atmos. Chem. Phys., 11, 1929-1948, doi:10.5194/acp-11-1929-2011, 2011.

Qian, Y., Wang, H., Zhang, R., Flanner, M. G., and Rasch, P. J.: A Sensitivity Study on Modeling Black Carbon in Snow and its Radiative Forcing over the Arctic and Northern China, Environ. Res. Lett., 9(6): Article No. 064001, doi:10.1088/1748-9326/9/6/064001, 2014a.

Qian, Y., Yasunari, T. J., Doherty, S. J., Flanner, M. G., Lau, W. K. M., Ming, J., Wang, H., Wang, M., Warren, S. G., and Zhang, R.: Light-absorbing Particles in Snow and Ice: Measurement and Modeling of Climatic and Hydrological impact, Adv. Atmos. Sci., doi: 10.1007/s00376-014-0010-0, 2014b, in press.

691 Ramanathan, V. and Carmichael, G.: Global and regional climate changes due to
692 black carbon, Nature Geoscience, 1, 221–227, 2008.

693 Ramanathan, V., Chung, C., Kim, D., Bettge, T., Buja, L., Kiehl, J. T., Washington,
694 W. M., Fu, Q., Sikka, D. R., and Wild, M.: Atmospheric brown clouds: impacts on
695 South Asian climate and hydrological cycle, Proc. Natl. Acad. Sci. USA, 102, 5326–
696 5333, 2005.

697 Ramanathan, V., Ramana, M. V., Roberts, G., Kim, D., Corrigan, C., Chung, C.,
698 Winker, D.: Warming trends in Asia amplified by brown clouds solar absorption,
699 Nature, 448, 575–578, 2007.

700 Reddy, M. S. and Venkataraman, C.: Inventory of aerosol and sulphur dioxide
701 emissions from India. Part II – biomass combustion, Atmos. Environ., 36, 699–712,
702 2002.

703 Revelle, R.: Energy use in rural India, Science, 192, 969–975, 1976.

704 Rienecker, M. M., Suarez, M. J., Gelaro, R., Todling, R., Bacmeister, J., Liu, E.,
705 Bosilovich, M. G., Schubert, S. D., Takacs, L., Kim, G.-K., Bloom, S., Chen, J.,
706 Collins, D., Conaty, A., da Silva, A., Gu, W., Joiner, J., Koster, R. D., Lucchesi, R.,
707 and Molod, A.: MERRA – NASA's Modern-Era Retrospective Analysis for Research
708 and Applications, J. Clim., 24, 3624–3648, 2011.

709 Sarka, S., Chokngamwong, R., Cervone, G., Singh, R. P., and Kafatos, M.: Variability
710 of aerosol optical depth and aerosol forcing over India, Adv. Space Res., 37, 2153–
711 2159, 2006.

712 Sathaye, J. and Tyler, S.: Transitions in household energy use in urban China, India,
713 the Philippines, Thailand, and Hong Kong, Annu. Rev. Energ. Environ., 16, 295–335,
714 1991.

715 Stone, E. A., Lough, G. C., Schauer, J. J., Praveen, P. S., Corrigan, C. E, and
716 Ramanathan, V.: Understanding the origin of black carbon in the atmospheric brown
717 cloud over the Indian Ocean, J. Geophys. Res., 112, D22S23,
718 doi:10.1029/2006JD008118, 2007.

719 Streets, D. G. and Waldhoff S. T.: Biofuel use in Asia and acidifying emissions,
720 Energy, 23, 1029–1042, 1998.

721 Tie, X., Wu, D., and Brasseur, G.: Lung cancer mortality and exposure to atmospheric
722 aerosol particles in Guangzhou, China, Atmos. Environ., 43, 2375–2377, 2009.

723 Venkataraman, C., Habib, G., Eiguren-Fernandez, A., Miguel, A. H., and Friedlander,
724 S. K.: Residential biofuels in South Asia: carbonaceous aerosol emissions and climate

impacts, Science, 307, 1454–1456, 2005.

Venkataraman, C., Sagar, A. D., Habib, G., Lam, N., and Smith, K. R.: The Indian National Initiative for advanced biomass cook-stoves: the benefits of clean combustion, Energy Sustain. Dev., 14, 63–72, 2010.

Wang, H., Easter, R. C., Rasch, P. J., Wang, M., Liu, X., Ghan, S. J., Qian, Y., Yoon, J.-H., Ma, P.-L., and Vinoj, V.: Sensitivity of remote aerosol distributions to representation of cloud–aerosol interactions in a global climate model, Geosci. Model Dev., 6, 765–782, doi:10.5194/gmd-6-765-2013, 2013.

Wang, H., Rasch, P. J., Easter, R. C., Singh, B., Zhang, R., Ma, P. L., Qian, Y., and Beagley, N.: Using an explicit emission tagging method in global modeling of source-receptor relationships for black carbon in the Arctic: Variations, Sources and Transport pathways, J. Geophys. Res.-Atmos., 119, doi:10.1002/2014JD022297, 2014.

Warren, S. G. and Wiscombe, W. J.: A model for the spectral albedo of snow. II: snow containing atmospheric aerosols, J. Atmos. Sci., 37, 2734–2745, 1980.

Wiscombe, W. J., and Warren, S. G.: A model for the spectral albedo of snow. I: Pure snow, J. Atmos. Sci., 37, 2712–2733, 1980.

Xu, B., Cao, J., Hansen, J., Yao, T., Joswiak, D. R., Wang, N.,Wu, G., Wang, M., Zhao, H., Yang, W., Liu, X., and He, J.: Black soot and the survival of Tibetan glaciers, Proc. Natl. Acad. Sci. USA, 106, 22114–22118, 2009a.

Xu, B., Wang, M., Joswiak, D. R., Cao, J., Yao, T., Wu, G., Yang, W., and Zhao, H.: Deposition of anthropogenic aerosols in a southeastern Tibetan glacier, J. Geophys. Res., 114, D17209, doi:10.1029/2008JD011510, 2009b.

Yang, M., Howell, S. G., Zhuang, J., and Huebert, B. J.: Attribution of aerosol light absorption to black carbon, brown carbon, and dust in China–interpretations of atmospheric measurements during EAST-AIRE, Atmos. Chem. Phys., 9, 2035-2050, doi:10.5194/acp-9-2035-2009, 2009.

Zhao, S., Ming, J., Sun, J., and Xiao, C.: Observation of carbonaceous aerosols during 2006–2009 in Nyainqêntanglha Mountains and the implications for glaciers, Environ. Sci. Pollut. Res., 20(8), 5827-5838, doi: 10.1007/s11356-013-1548-6, 2013a.

Zhao, Z., Cao, J., Shen, Z., Xu, B., Chen, L-W. A., Ho, K., Han, Y., Zhu, C., and Liu, S.: Aerosol particles at a high-altitude site on the Southeast Tibetan Plateau, China: implications for pollution transport from South Asia, J. Geophys. Res.-Atmos., 118, 11360–11375, doi:10.1002/jgrd.50599, 2013b.

759 Table 1. Source regions (South Asia, East Asia, Southeast Asia, and Central Asia) and corresponding BC emissions (Tg a^{-1}) and
760 fractional contributions (%) to BC deposition flux at the Zuoqiupu site in monsoon (June-September), non-monsoon (October-May),
761 and all months during 1996-2005.

Source Regions	Latitude	Longitude	Monsoon		Non-monsoon		Annual	
			Contribution	Emission	Contribution	Emission	Contribution	Emission
South Asia	5-35°N	50-95°E	38.51	0.65	81.26	0.74	74.48	0.71
East Asia	15-50°N	95-150°E	56.24	1.75	13.91	1.90	20.66	1.85
Southeast Asia	0-15°N	95-130°E	0.05	0.28	0.16	0.33	0.15	0.31
Central Asia	35-50°N	50-95°E	2.62	0.11	0.86	0.09	1.14	0.10

762

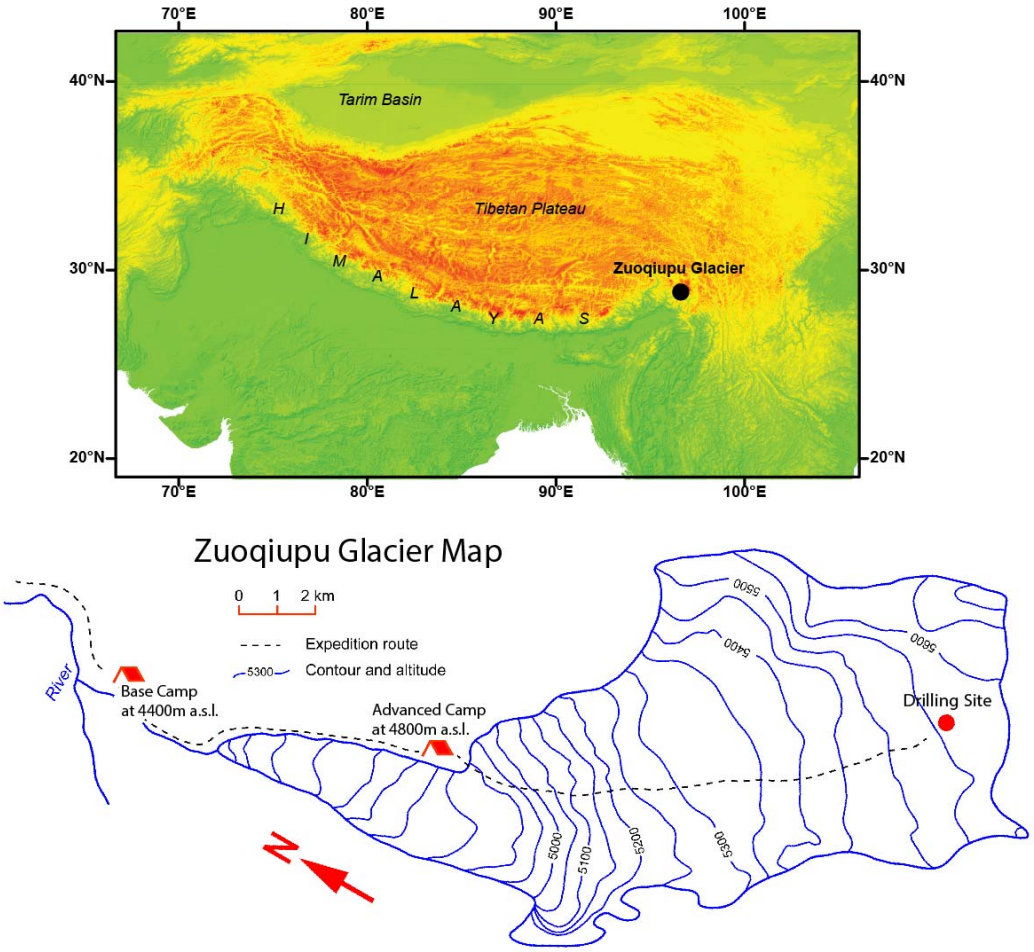

763

764 Figure 1. Site location of Zuoqiupu Glacier (top): black circle represents the location of
765 Zuoqiupu Glacier, and warm colors indicate high elevations over the Tibetan Plateau.
766 Detailed elevation contours of the Zuoqiupu Glacier are shown in the bottom panel. Red
767 circle marks the ice core drill site.

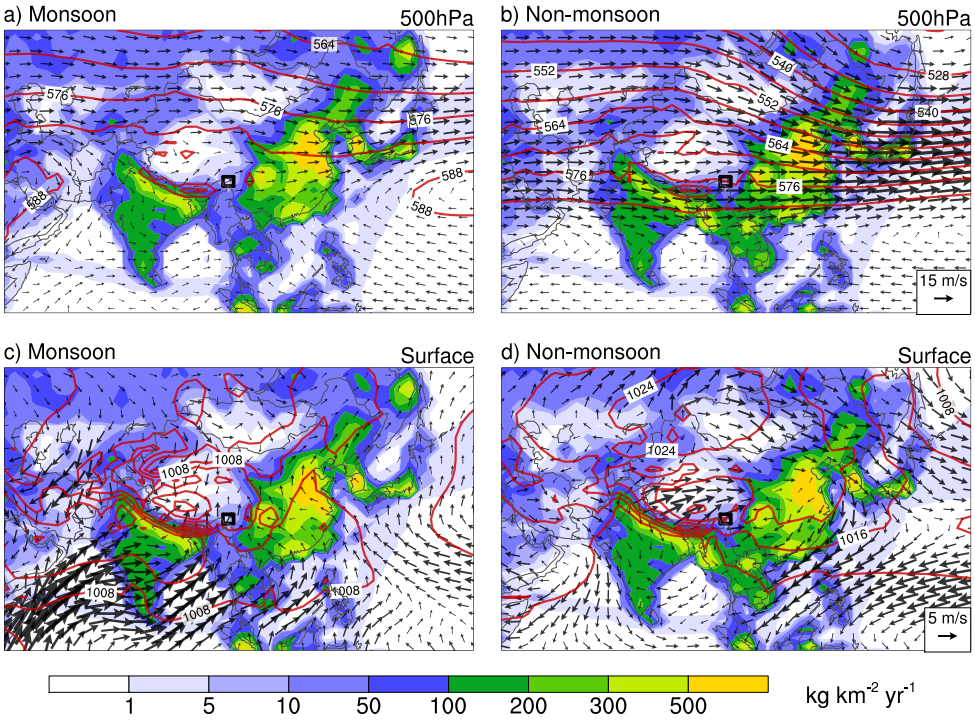

768

769 Figure 2. 10-year (1996-2005) mean wind vectors (denoted by arrows) at 500hPa (a, b)
770 and the surface (c, d) during summer monsoon (June-September; a, c) and non-monsoon
771 season (October-May; b, d) from MERRA reanalysis datasets used to drive the CAM5
772 simulation. 500 hPa Geopotential height (units: 10 m) contours with an interval of 60 m
773 and mean sea-level pressure (units: hPa) contours with an interval of 4 hPa are
774 superimposed on panels (a, b) and (c, d), respectively. The background colors show mean
775 BC emission rates based on the IPCC present-day scenario for the corresponding months.
776 The small black box marks the model grid-cell in which the ice core drill site resides.

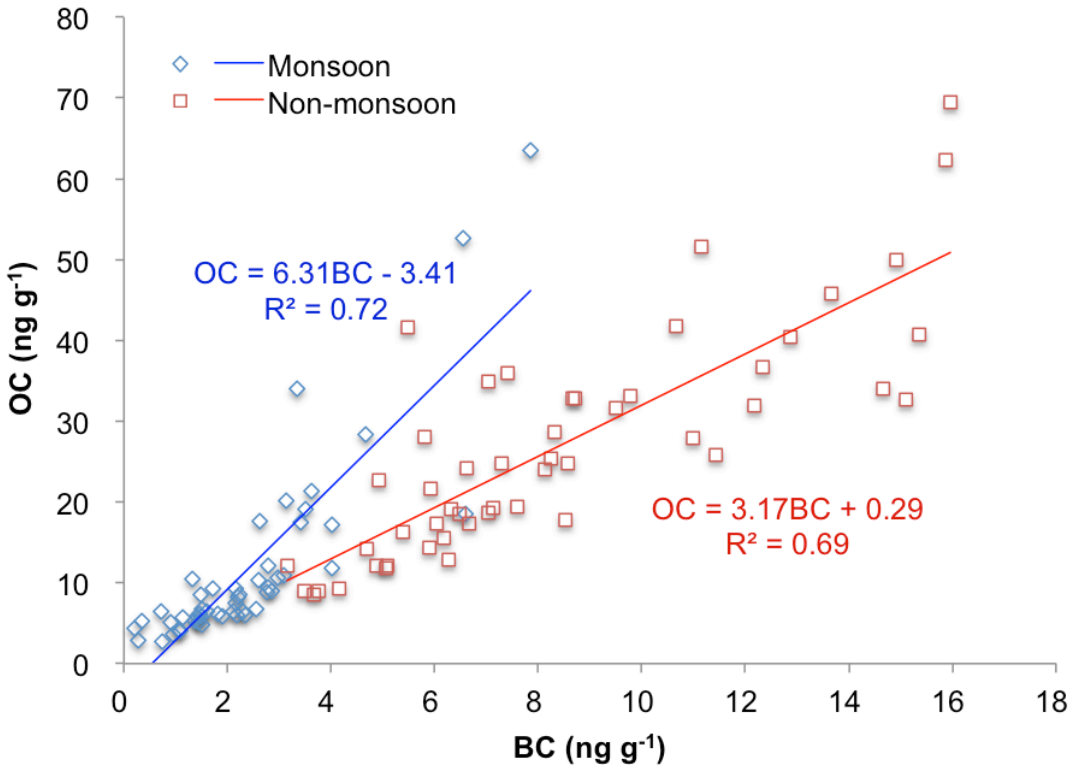

777

778 Figure 3. Scatter plots for yearly monsoon and non-monsoon mean OC and BC
779 concentrations during 1956-2006, obtained from the ice core measurements, and
780 corresponding linear regressions.

781

782

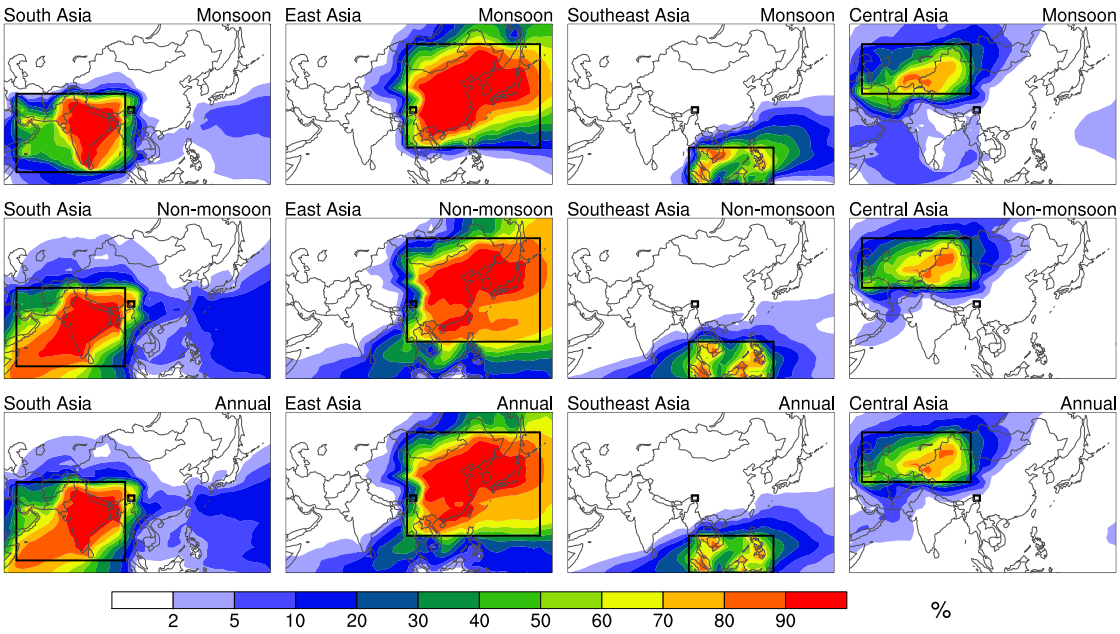

783 Figure 4. Spatial distributions of fractional contribution from the four source regions
784 (South Asia, East Asia, Southeast Asia, and Central Asia) to monsoon, non-monsoon, and
785 annual mean BC deposition fluxes during 1996-2005. The large black boxes indicate the
786 boundary of source regions, and the small black box marks the model grid-cell where the
787 Zuoqiupu drill site is located.

788

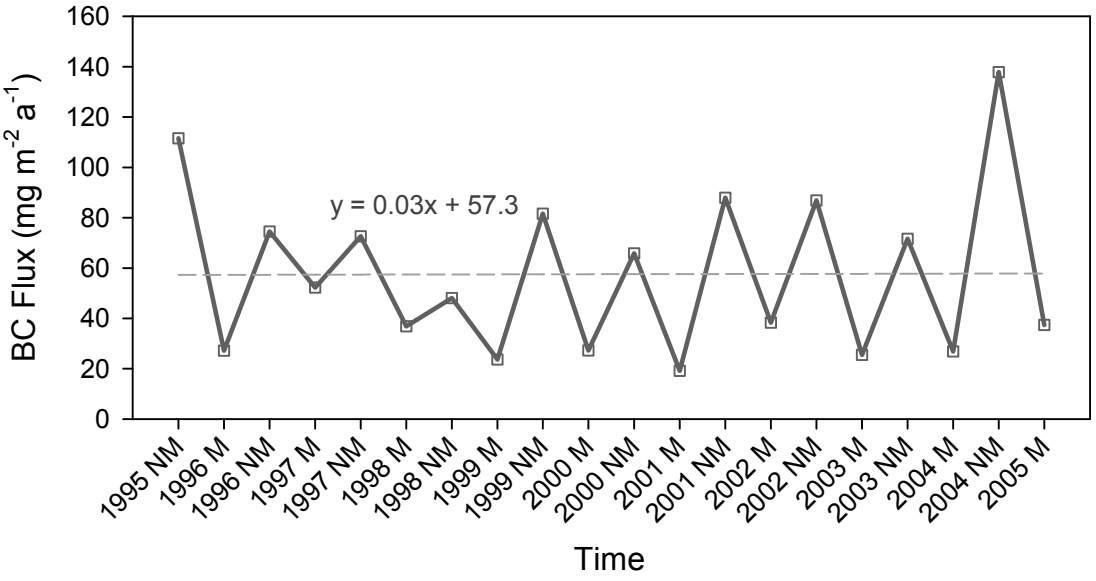

789

790 Figure 5. Seasonal dependence ("NM" for non-monsoon and "M" for monsoon season).
791 of BC deposition flux at the Zuoqiupu site from 1995 to 2005 simulated in CAM5. The
792 dash line represents a linear regression of all data points.

793

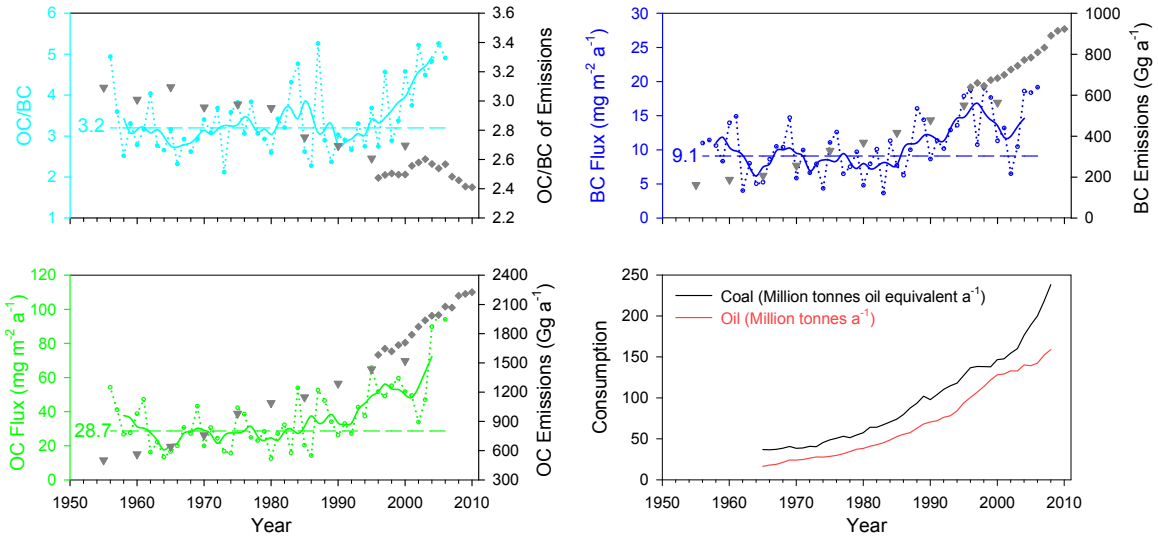

794

795 Figure 6 Time series of annual (dotted line with circles) and 5-year averaged (solid line)
796 OC/BC ratios (top-left), BC (top-right) and OC deposition fluxes (bottom-left) in the
797 Zuoqiupu ice core for the time period of 1956-2006. The average values of OC/BC ratio,
798 BC and OC during 1956-1979 are marked by dashed lines. BC and OC emissions in
799 South Asia (Bond et al., 2007) and corresponding OC/BC emission ratios are illustrated
800 with gray triangles, and with gray diamonds for emissions in India (Lu et al., 2011). Coal
801 and oil consumption data are shown in the bottom-right panel (BP Group, 2009).